



Ag particles modified Cu_xO ($x = 1, 2$) nanowires on nanoporous Cu-Ag bimetal network for antibacterial applications

Chunling Qin, Mengmeng Zhang, Baoye Li*, Yongyan Li, Zhifeng Wang*

School of Materials Science and Engineering, Hebei University of Technology, Tianjin 300130, China

ARTICLE INFO

Article history:

Received 13 August 2019

Received in revised form 28 September 2019

Accepted 15 October 2019

Available online 16 October 2019

Keywords:

Amorphous materials

Corrosion

Nanoporous

Anodizing

Bimetal

ABSTRACT

Nano-sized bimetal, bimetallic oxides and their composites have aroused widespread research interests because of their multifunctional performances. The development of their novel structures and synthesis techniques is urgently needed. Herein, we fabricated a novel Ag nanoparticles modified Cu_xO ($x = 1, 2$) nanowires on nanoporous copper-silver network ($\text{Ag}/\text{Cu}_x\text{O}@NP\text{-CuAg}$) with hierarchical porous structure through dealloying and anodizing process. Nanoporous CuAg bimetal network (NP-CuAg), prepared by dealloying of $\text{Cu}_{40}\text{Zr}_{50}\text{Ag}_{10}$ metallic glass (MG) ribbon, was used as the anodizing substrate to provide bimetal sources for the first time. Then Ag nanoparticles modified Cu_xO ($x = 1, 2$) nanowires were synthesized on NP-CuAg network by anodizing and calcination. Due to the unique structure and the synergistic effect of Cu and Ag elements, the as-obtained composite presents good antibacterial activity and a wide application prospect as a multifunctional material.

© 2019 Elsevier B.V. All rights reserved.

1. Introduction

Nanostructured metals and metallic oxides have been greatly used in many fields, due to the unique structural characteristics and a series of novel properties [1–4]. Up to now, a variety of nanostructures has been fabricated, such as nanofibers, nanospheres, nanorods, nanoparticles, and nanowires [5–9]. Currently, bimetal Cu-Ag or oxides nanocomposites have caused widespread interest because of their multifunctional performances. The combination of nanostructures with diversified shapes and components, such as Ag nanoparticles/CuO nanofibers [10] and $\text{Ag}/\text{Cu}_2\text{O}$ nanoparticles [11], enhanced their intrinsic characteristics and properties. Nevertheless, the preparation techniques are complex and time consuming. Therefore, it is urgent to develop a facile method for developing Cu-Ag oxide composites with novel nanostructures.

This work introduces a simple synthesis approach of dealloying followed by anodizing to fabricate Cu_xO ($x = 1, 2$) nanowires modified by Ag nanoparticles grown on nanoporous Cu-Ag network ($\text{Ag}/\text{Cu}_x\text{O}@NP\text{-CuAg}$). The nanoporous bimetal CuAg network (NP-CuAg), obtained by dealloying $\text{Cu}_{40}\text{Zr}_{50}\text{Ag}_{10}$ metallic glass (MG) ribbon, was used as the anodizing substrate. The anodizing technique is performed on NP-CuAg network to form Cu_xO ($x = 1, 2$) nanowires with coexisting Ag nanoparticles. The work provides

a new idea of synthesizing a multi-component material with multi-shaped nanostructures. Moreover, the antibacterial activity of $\text{Ag}/\text{Cu}_x\text{O}@NP\text{-CuAg}$ composites is also examined.

2. Experimental

The schematic formation process of $\text{Ag}/\text{Cu}_x\text{O}@NP\text{-CuAg}$ is shown in Fig. 1a. Firstly, $\text{Cu}_{40}\text{Zr}_{50}\text{Ag}_{10}$ (at.%) MG ribbons were prepared by melt-spinning technique [7]. Secondly, the ribbon was dealloyed [7,12] in 0.25 M HF solution for 6 h at 298 K to form the NP-CuAg network. Then anodizing method [13] was performed on DC Power Supply (TPR-12010D), with a NP-CuAg ribbon as working electrode and a platinum mesh as counter electrode in 0.5 M KOH solution at the constant current density of 10 mA/cm^2 for 5 or 7 min. Finally, the anodized ribbons were washed in deionized water and then calcined for 2 h at 473 K.

The phase was examined by X-ray diffraction (XRD, Bruker D8, Cu-K α) and X-ray photoelectron spectroscopy (XPS, Thermo Fisher Scientific). The structure was detected by scanning electron microscopy (SEM, Hitachi S-4800, 15 keV) equipped with EDS analysis and transmission electron microscopy (TEM, JEOL JEM-2010F, 200 keV).

The antibacterial activities of $\text{Ag}/\text{Cu}_x\text{O}@NP\text{-CuAg}$ composites were determined against *Escherichia coli* (*E. coli*). All composites and blank control samples are tested under the same conditions. The antibacterial properties were investigated by colony-count

* Corresponding authors.

E-mail addresses: libaoe@hotmail.com (B. Li), wangzfh@hebut.edu.cn (Z. Wang).

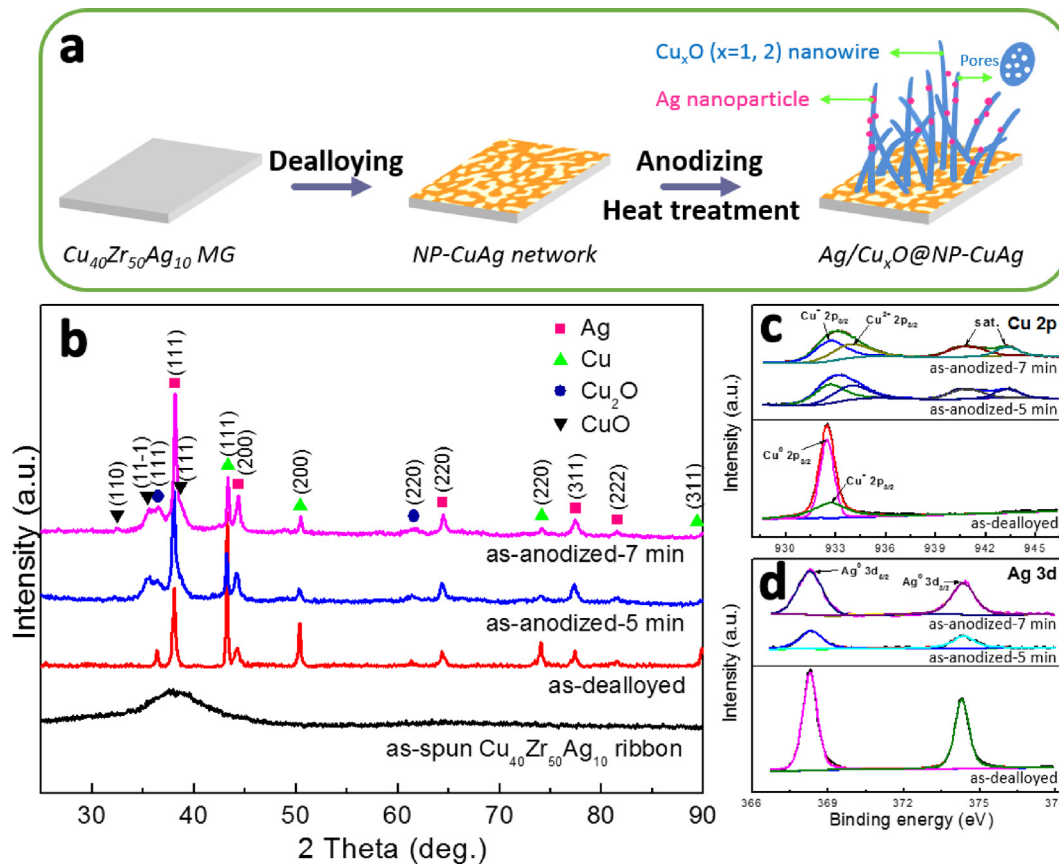


Fig. 1. (a) Schematics of formation process of Ag/Cu_xO@NP-CuAg composite. (b) XRD patterns of as-spun, as-dealloyed and as-anodized specimens. XPS spectra of as-dealloyed and as-anodized specimens: (c) Cu 2p, (d) Ag 3d.

method and the number of colonies was averaged on three petri dishes.

3. Results and discussion

Fig. 1b shows the XRD patterns of as-spun Cu₄₀Zr₅₀Ag₁₀ ribbon, as-dealloyed ribbon and as-anodized products for 5 and 7 min. The pattern of as-spun Cu₄₀Zr₅₀Ag₁₀ ribbon displays a broad peak, confirming an amorphous structure. The pattern of as-dealloyed ribbon exhibits distinct crystalline peaks of fcc Cu (JCPDS No.04-0836), fcc Ag (JCPDS No.04-0783) and minor Cu₂O (JCPDS No.05-0667), indicating Zr element dissolved into HF solution and Cu and Ag retained. After anodizing, there are several peaks in the XRD pattern which match with the (111), (110) and (11-1) planes of CuO (JCPDS #48-1548) [13]. Meanwhile, the Ag and Cu₂O peaks of as-anodized specimens are much higher than those of as-dealloyed specimen, indicating that the contents of Ag and Cu₂O increase after anodizing. In addition, the Cu 2p XPS spectra of as-dealloyed and as-anodized specimens are further shown in Fig. 1c. For as-dealloyed specimen, the peak at 932.46 eV is assigned to Cu 2p_{3/2} of metallic Cu, and the peak at 934.7 eV (Cu⁺) is from cuprous oxides (slight oxidation of copper in air). After anodizing, the peaks are located at 932.8 eV and 933.8 eV accompanying with two satellite peaks, confirming the existence of Cu²⁺ and Cu⁺. The Ag 3d_{5/2} and Ag 3d_{3/2} peaks (Fig. 1d) located at 368.3 eV and 374.3 eV, respectively, are corresponded to the metallic state Ag for all the specimens. XPS analysis is consistent with XRD results.

Fig. 2a displays the surface morphology of as-dealloyed ribbon and the inset corresponding EDS results. The as-dealloyed ribbon,

consisting only of Cu and Ag elements, shows a bi-continuous and interconnected porous network structure, indicating the NP-CuAg is formed. Then, NP-CuAg is used as anodizing substrate to provide bimetal sources. In Fig. 2b, a good deal of nanowires distribute on the surface of NP-CuAg network after anodizing for 5 min. The nanowire is about 25–35 nm in diameter and up to micrometer scale in length. It is carefully seen that many scattered nanoparticles are located on the nanowires in the inset in Fig. 2b at higher magnification. From the cross-sectional image of the as-anodized ribbon for 5 min shown in Fig. 2c, it is found that nanowires with the thickness of ~5.7 μm grow uniformly on the NP-CuAg substrate. Moreover, the interface between nanowires and substrate shows a tight junction. When the anodizing time extends to 7 min (Fig. 2d), it appears that the nanowires become thickened accompanied by the size of Ag nanoparticles increasing.

The microstructure of as-anodized ribbon for 5 min was further examined by TEM detection in Fig. 3. The bright-field TEM image of nanowires is shown in Fig. 3a. There are a mass of nanopores with small size of 1.5–2.5 nm which distribute on the each nanowire. Meanwhile, the scattered nanoparticles with sizes of 12–13 nm in diameter attach to the nanowire. The inset of Fig. 3a shows selected area electron diffraction (SAED) pattern of anodized products. The diffraction rings match with fcc Ag, monoclinic CuO and cubic Cu₂O. Combining with the lattice fringes in Fig. 3b, it can be identified that the component of nanoparticles is Ag metal, while the nanowires are composed of CuO and Cu₂O. Fig. 3c–g show the TEM-EDS mapping results of the composite. From Fig. 3e and f, it is found that Cu and O elements uniformly distribute through the nanowires, whereas Ag elements aggregate to form

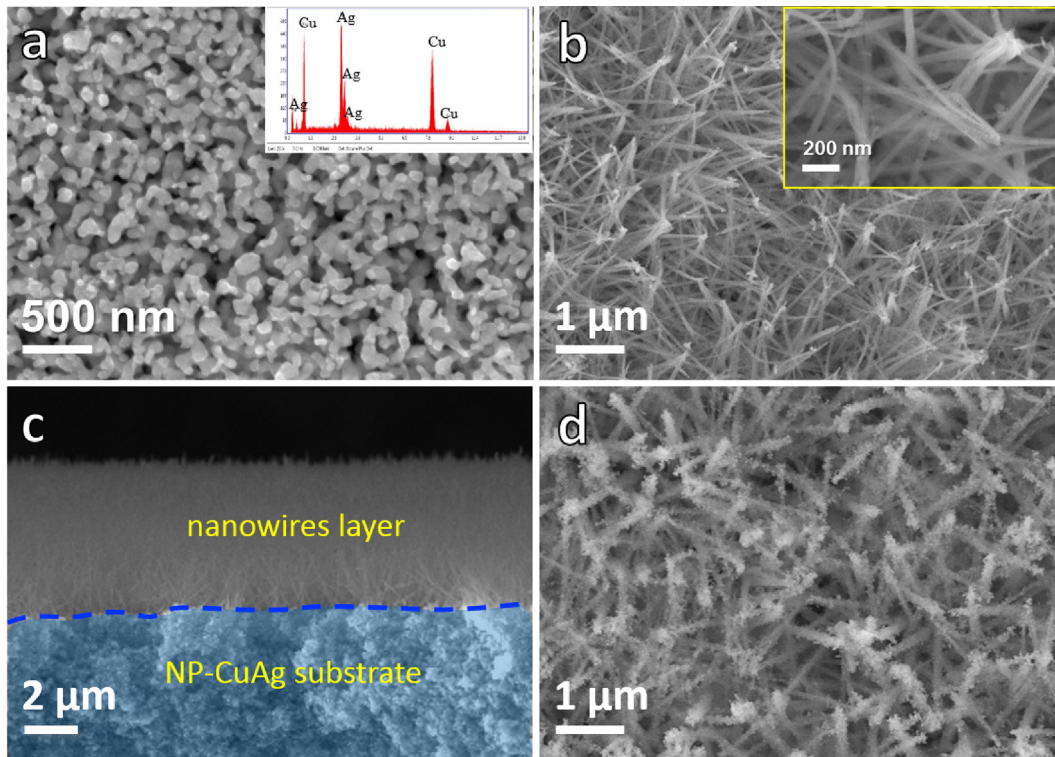


Fig. 2. (a) Surface morphology of the NP-CuAg substrate and the inset of corresponding EDS result. (b) SEM image of as-anodized product for 5 min and the inset of higher magnification. (c) The cross-sectional image of as-anodized specimen for 5 min. (d) Surface morphology of as-anodized product for 7 min.

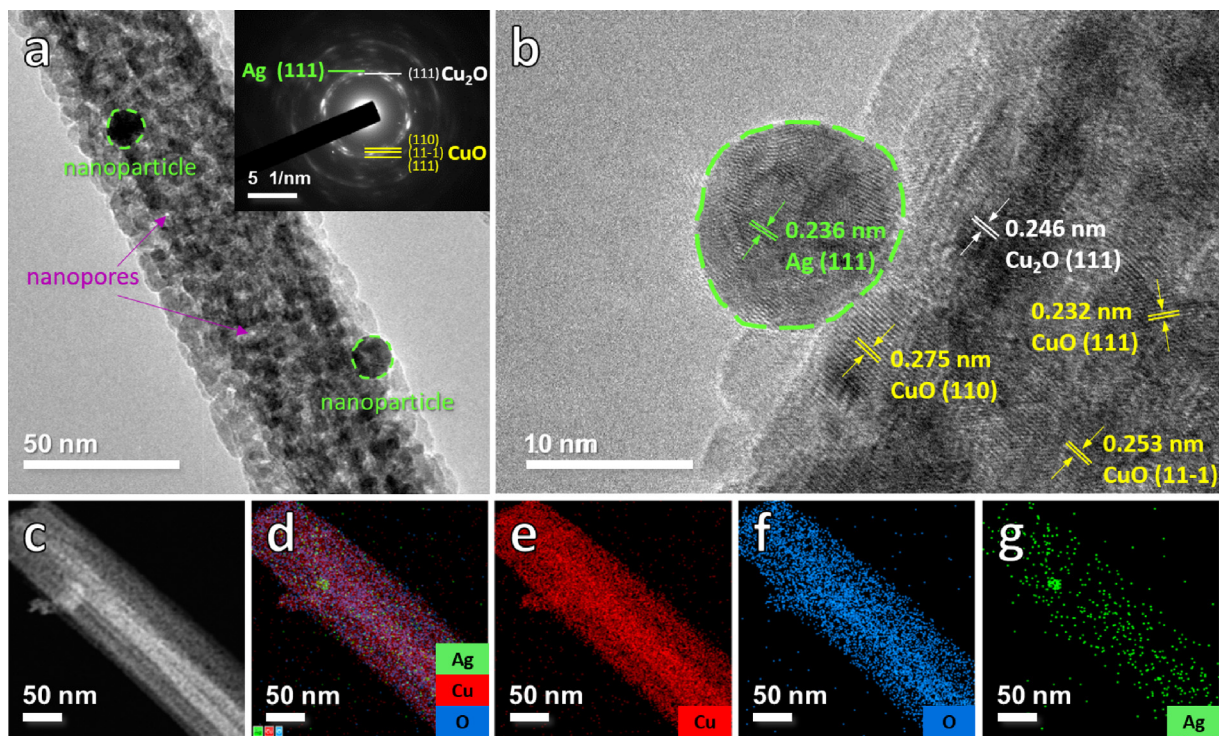


Fig. 3. (a) TEM image, SAED of inset in (a), (b) HRTEM image, (c)–(g) TEM-EDS mapping of the nanowire accompanying with nanoparticles anodized for 5 min.

nanoparticles (Fig. 3g), which is in good agreement with the TEM results. From above results, it can be concluded that the Ag/Cu_xO@NP-CuAg composites are successfully fabricated. Moreover, the present composites have a hierarchical nanopor-

ous structure, i.e. containing the macropores among nanowires twining space and nanopores on NP-CuAg network.

The optical images of *E. coli* colonies incubated on the blank control sample, Ag/Cu_xO@NP-CuAg (anodized for 5 and 7 min) for

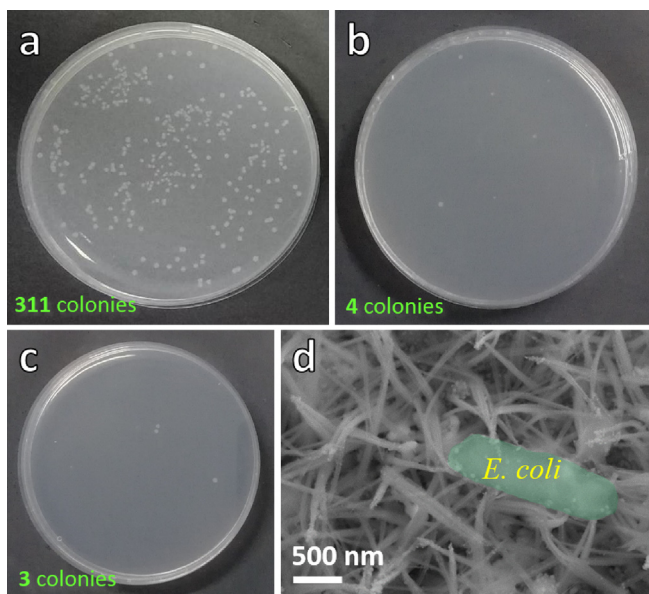


Fig. 4. Optical images of *E. coli* colonies incubated for 12 h on (a) the blank control sample, (b) Ag/Cu_xO@NP-CuAg (5 min) and (c) Ag/Cu_xO@NP-CuAg (7 min). (d) SEM image of Ag/Cu_xO@NP-CuAg (5 min) after bacteriostatic test for 12 h.

12 h are shown in Fig. 4a–c, respectively. It is clearly observed that there are almost no colonies in Fig. 4b and c as compared to that in Fig. 4a, revealing the coexistence of Cu_xO and Ag nanoparticles is effective for inhibiting the growth of *E. coli*. Additionally, we can clearly see that the microstructure of Ag/Cu_xO@NP-CuAg (5 min) after bacteriostatic test for 12 h (Fig. 4d) still keeps similar morphology. Hence, the composites exhibit excellent antibacterial activities. All in all, the novel Ag/Cu_xO@NP-CuAg composites with a peculiar and multi-component microstructure will have a broad application prospect in many fields. More performance investigation will be discussed in detail in future.

4. Conclusions

A simple fabrication strategy is applied to synthesize the multi-component Ag/Cu_xO@NP-CuAg composites with hierarchical nanoporous structure by dealloying and anodizing strategy. The Cu_xO ($x = 1, 2$) nanowires with coexisting Ag nanoparticles in-situ grow uniformly on NP-CuAg network, which provides bimetal sources for potential multifunctional performances. The new-developed Ag/Cu_xO@NP-CuAg composites demonstrate excellent antibacterial activity and will show a wide application prospect in many fields. The work also provides us a novel idea for synthesizing other bimetal/bimetallic oxides composites.

Declaration of Competing Interest

The authors declare that they have no known competing financial interests or personal relationships that could have appeared to influence the work reported in this paper.

Acknowledgments

This work is financially supported by the National Natural Science Foundation of China (51671077).

References

- [1] A.M. Allahverdiyev, E.S. Abamor, M. Bagirova, et al., *Future Microbiol.* 6 (2011) 933–940.
- [2] L.H. Zhang, X.F. Wang, *Appl. Phys. A* 117 (2014) 2189–2196.
- [3] X.Y. Lang, A. Hirata, T. Fujita, et al., *Nat. Nanotechnol.* 6 (2011) 232–236.
- [4] X.B. Li, S.Y. Ma, F.M. Li, et al., *Mater. Lett.* 100 (2013) 119–123.
- [5] H. Wu, L.B. Hu, M.W. Rowell, et al., *Nano Lett.* 10 (2010) 4242–4248.
- [6] D.M. Zhu, C.Q. Xia, Z.D. Yang, et al., *Mater. Lett.* 245 (2019) 49–52.
- [7] D.H. Zheng, F. Zhao, Y.Y. Li, et al., *Electrochim. Acta* 297 (2019) 767–777.
- [8] P.X. Zhao, N. Li, D. Astruc, *Coord.Chem. Rev.* 257 (2013) 638–665.
- [9] Z.F. Wang, Y.S. Zhang, H.Q. Xiong, et al., *Sci. Rep.* 8 (2018) 6530.
- [10] B.Z. Zhang, G.Y. Liu, A.W. Yao, et al., *Sensor Actuat. B* 195 (2014) 431–438.
- [11] F.R. Juang, W.C. Chern, *Mat. Sci. Semicon. Proc.* 101 (2019) 156–163.
- [12] X. Wang, R. Li, Z. Li, et al., *J. Mater. Chem. B* 7 (2019) 4169–4176.
- [13] M. Li, Y.Y. Li, Q. Zhang, et al., *Appl. Surf. Sci.* 483 (2019) 285–293.